BIOCHEMISTRY
including biophysical chemistry & molecular biology

Article

pubs.acs.org/biochemistry

Role of the Ectodomain Serine 275 in Shaping the Binding Pocket of the ATP-Gated P2X3 Receptor

Nataliia Petrenko,[†] Kamil Khafizov,[‡] Vendula Tvrdonova,[§] Andrei Skorinkin,[∥,⊥] and Rashid Giniatullin*[,†]

[†]Department of Neurobiology, A. I. Virtanen Institute, University of Eastern Finland, Kuopio, Finland, and [‡]Computational Structural Biology Group, Max Planck Institute of Biophysics, 60438 Frankfurt am Main, Germany

[§]Department of Cellular and Molecular Neuroendocrinology, Institute of Physiology, Academy of Sciences of the Czech Republic, Prague, Czech Republic

[∥]Kazan Federal University, Kazan, Russia

[⊥]Kazan Institute of Biochemistry and Biophysics, Kazan, Russia

Supporting Information

ABSTRACT: ATP-activated P2X3 receptors expressed in nociceptive sensory neurons play an important role in pain signaling. Basic properties of this receptor subtype, including very strong desensitization, depend on the rate of dissociation of the agonist from the binding site. Even though the rough structure of the ATP binding site has been proposed on the basis of the X-ray structure of the zebrafish P2X4 receptor and mutagenesis studies, the fine subunit-specific structural properties predisposing the receptor to tight capture of the agonist inside the binding pocket have not been elucidated. In this work, by exploring in silico the functional role for the left flipper located in the ectodomain region, we identified within this loop a candidate residue S275, which could contribute to the closure of the agonist-binding pocket. Testing of the S275 mutants using the patch−clamp technique revealed a crucial role for S275 in agonist binding and receptor desensitization. The S275A mutant showed a reduced rate of onset of desensitization and accelerated resensitization and was weakly inhibited by nanomolar agonist. Extracellular calcium application produced inhibition instead of facilitation of membrane currents. Moreover, some full agonists became only partial agonists when applied to the S275A receptor. These effects were stronger with the more hydrophobic mutants S275C and S275V. Taken together, our data suggest that S275 contributes to the closure of the agonist-binding pocket and that effective capture of the agonist provided by the left flipper in calcium-dependent manner determines the high rate of desensitization, slow recovery, and sensitivity to nanomolar agonist of the P2X3 receptor.

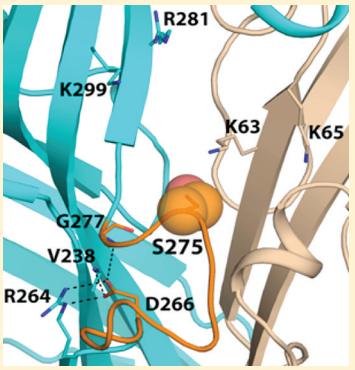

Peripheral ATP-activated ion channels (P2X receptors) play a crucial role in the mechanisms of pain sensation following tissue injury or inflammation.[1−3] Of seven subtypes of P2X receptors, the P2X3 subtype expressed in nociceptive sensory neurons is specifically designed for transmission of pain signals.[1] One of the key issues related to the function of P2X receptors is the location and structure of the agonist binding site. Recently, the structure of the ATP binding site within the P2X receptors has been roughly elucidated on the basis of the available X-ray structure of the zebrafish P2X4 receptor.[4] These new data are consistent with previous descriptions of residues obtained from a mutagenesis approach, which indicated a key contribution to ATP phosphate binding by residues K68, K70, R292, and K309 [P2X1 numbering (reviewed in refs 3, 5, and 6)], while the adenine ring may interact with sites located between residues F185 and T186 and residues N290 and F291.[7] Furthermore, for the human P2X3 receptor, residues K63, G66, T172, K176, N177, N279, R281, K284, R281, R295, and K299 were important for providing a full agonist response.[8]

Because the X-ray structure of the P2X receptor became available, homology models of various ATP-gated receptors were published,[8−13] which contributed greatly to our understanding of P2X receptor function. An important structure within the ectodomain of P2X receptors, first described in the crystal structure of the P2X4 receptor, is the so-called "left flipper".[4] In the P2X3 receptor, this left flipper contains amino acid residue D266 that virtually determines the sensitivity of the P2X3 receptor to extracellular calcium ions known as strong allosteric modulators of P2X3 receptor responses.[14−16] Unlike P2X3 receptors that are facilitated by calcium ions,[14] P2X2 receptors are inhibited by these cations.[17] Another basic difference between P2X2 and P2X3 receptors is the fact that the former are insensitive to the agonist α,β-meATP.[18] This fact presumes that there should be subunit-specific arrangements of the binding site of the P2X3 receptor. However, the precise subunit-specific conformation of the binding site requires further studies especially because the current model describes only the closed conformation available for a single type of P2X receptor. In this regard, a very recent study based on action of a

Received: May 26, 2011
Revised: August 17, 2011
Published: August 31, 2011

thiol-reactive agonist identified two new residues (N140 and L186) as important contributors to the ATP binding site in the P2X2 receptor.[13] In all these studies, the most attention was paid to receptors containing the P2X1, P2X2, and P2X4 subunits.[5] Another member of this family, the P2X3 receptor, is known to be activated by many full agonists with different chemical structures.[19,20] Furthermore, the P2X3 receptor subtype is characterized by slow dissociation of the agonist, especially from the desensitized receptor state.[21] Therefore, in the P2X3 receptor, the binding site could have specific structural properties predisposing it to tight closure and/or capture of the ligand inside the binding pocket to prevent fast dissociation of the agonist.

Desensitization often complicates the evaluation of potency in structure−function studies. For instance, the altered potency of the P2X3 subtype is not always a result of pure changes in agonist binding but could simply indicate attenuation or augmentation of the onset of desensitization.[22] In the P2X3 receptor, desensitization is affected by mutations of residue D266, which also determines the agonist activity of certain full agonists such as the stable ATP analogue α,β-meATP.[16] However, no mechanistic interpretation of these pre-X-ray receptor structure findings has been offered to date. Therefore, in this work, we constructed a homology model of the rat P2X3 receptor on the basis of a recently published X-ray structure of the zebrafish P2X4 receptor.[4] Using this model and sequence analysis of the rat P2X receptors, we propose a role for the D266 residue, located in the left flipper region, as a stabilizer of the position of a loop potentially involved in binding some of the agonists. Furthermore, we identified a new residue, S275, that according to in silico trials should be an important determinant in forming the agonist-binding pocket in the P2X3 receptor. Experimental testing revealed that the S275 mutant indeed had functional properties that were similar to those previously observed with the D266A mutant located nearby, within the same left flipper.[16] Substitution of serine with more hydrophobic residues, cysteine and valine, disrupted the function of the binding site even more than alanine substitution, proportional to their hydropathy indexes. In this work, potential changes in the agonist binding and gating were also evaluated with kinetic modeling, which provided a rationale for the modified properties of mutant receptors.

Our data are consistent with the view that although the basic structure of the binding site is expected to be similar for all subtypes of P2X receptors, the fine arrangement of the agonist binding region in the left flipper, including an important contribution from D266 and S275, determines the high rate of desensitization and promiscuous properties of the P2X3 receptor. Thus, S275 represents a newly identified residue that significantly contributes to the specific properties of the P2X3 receptor subtype.

EXPERIMENTAL PROCEDURES

Plasmids. The rat P2X3 gene (a gift from S. S. Stojilkovic) was subcloned into pIRES2-EGFP (Clontech, Mountain View, CA). Single-point mutant receptors were constructed by polymerase chain reaction amplification using specific overlapping oligonucleotide primers (synthesized by VBC-Genomics, Vienna, Austria), the QuikChange II site-directed mutagenesis kit (Stratagene, La Jolla, CA), and P2X3/pIRES2-EGFP as the template. The sequence of the construct was verified.

Electrophysiological Recordings. HEK293 cells were transfected using FuGENE HD Transfection Reagent (Roche, Helsinki, Finland). Recordings from HEK cells were made in the whole cell configuration using the HEKA PC-10 amplifier (HEKA Elektronik). Cells were continuously superfused (3 mL/min) with the physiological solution containing 152 mM NaCl, 5 mM KCl, 1 mM $MgCl_2$, 2 mM $CaCl_2$, 10 mM glucose, and 10 mM HEPES (pH adjusted to 7.4 with NaOH). Patch pipettes had a resistance of 4−5 MΩ when filled with 130 mM CsCl, 10 mM HEPES, 5 mM EGTA, 0.5 mM $CaCl_2$, 5 mM $MgCl_2$, 5 mM KATP, and 0.5 mM NaGTP (pH adjusted to 7.2 with CsOH). The osmolarity of the intracellular solution was ∼290 mOsm. EGFP-expressing single HEK cells illuminated with the xenon lamp were identified using a fluorescent inverted Olympus IX-71 microscope with specific optical filters and used for the current recordings (voltage-clamped at −70 mV). The data were analyzed off-line using FitMaster (HEKA Elektronik) and Origin version 8.0 (Microcal, Northampton, MA).

Drug Delivery. The following P2X3 agonists (obtained from Sigma-Aldrich, Helsinki, Finland) were diluted with the physiological solution to a final concentration before the experiment: α,β-methyleneATP (α,β-meATP), β,γ-methyleneATP (β,γ-meATP), ATP, and 2-methylthio-ATP (2MeS-ATP). Applications of agonists (exchange time of 20−40 ms) to the cell were performed with the rapid superfusion system (Rapid Solution Changer RSC-200, BioLogic Science Instruments, Grenoble, France). Unless otherwise indicated, the agonists were applied every 5−6 min to minimize receptor desensitization.

Homology Modeling. The three-dimensional structural model of the rat P2X3 receptor was built using Modeller9v5.[23] Calculations were based on the crystal structure of the zebrafish P2X4 receptor.[4] The sequences of rat P2X3 and zebrafish P2X4 receptors were aligned using AlignMe[24] with small manual modifications. The sequence alignment is shown in Figure S1 of the Supporting Information. The level of sequence identity between modeled regions of these two proteins is ∼45%, which is considered to be high enough to construct reliable homology models.[25] One thousand models were generated, and their quality was assessed using PROCHECK.[26] A single model was chosen for analysis on the basis of its low molpdf value and a high percentage of residues falling into the allowed region on a Ramachandran plot.

Multiple-sequence alignment was generated with T-Coffee.[27]

Kinetic Modeling. We have used the computer simulation method that is based on the solving of ordinary differential equations[28] composed on the ground of mass action law:

$$\frac{d\bar{P}(t)}{dt} = \bar{P}(t) \times \mathbf{Q}$$

where $\bar{P}(t)$ is the vector of the probability of existence of the receptor channel complex in different states at time t and $\mathbf{Q}$ is the matrix of transitions between states. We have used for our kinetic model of the P2X3 receptor the formerly developed cyclic scheme with the possibility of desensitization without opening:[29]

Scheme 1

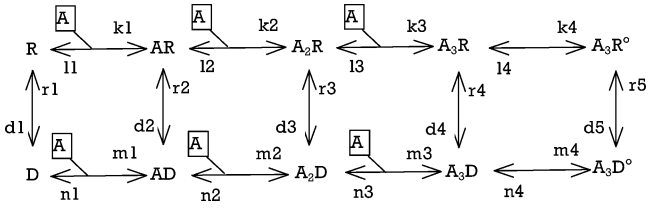

where A is the agonist and R, D, and R° are the $P2X_3$ receptor in the resting, desensitized, and open states, respectively. Rate constants are labeled near the corresponding transitions. The program was written in Pascal to solve numerically this set of differential equations using the eight-order Runge−Kutta method. The membrane current can be calculated by the following equation:

$$I(t) = (V - V_{eq})N \times P_{open}(t) \times \sigma$$

where V is the membrane potential, V_{eq} is the equilibrium potential, N is the total quantity of channels in the membrane, $P_{open}(t)$ is the probability of the open state ($A_3R°$) at time t, and σ is the single-channel conductance. If V, V_{eq}, N, and σ are constants, then the current at every moment is proportional to the total open channel probability. In this case, all parameters (rise time, recovery rate, EC_{50}, etc.) can be found by $P_{open}(t)$ analysis.

Data Analysis. Data are presented as the means ± standard error of the mean (n is the number of cells). The statistical significance was assessed with a Student's t test for parametric data or a Mann−Whitney rank sum test for nonparametric data, and using GraphPad Prism 4.03 (GraphPad Software Inc.) or Origin version 8.0 (Microcal). A P value of <0.05 was accepted as being indicative of a significant difference. In experiments with the paired-pulse agonist applications, we constructed the curves for recovery from desensitization using the following fitting function:

$$y = y_0 + Ae^{-(x-x_0)/\tau}$$

where τ is the decay time constant for recovery. τ values obtained from fitting of recovery in individual cells expressing wild-type (WT) or mutant receptors were compared using an unpaired t test. Notably, the comparison of recovery rates for β,γ-meATP between the WT and S275A receptors was hampered by the fact that in the S275A mutant desensitization was minimal at the end of agonist application.

RESULTS

Homology Modeling of the Rat P2X3 Receptor and Sequence Analysis. Because we previously found that agonist binding and desensitization largely depend on a negatively charged D266 residue in the left flipper region,[16] we first aimed to provide a mechanistic explanation for the role of D266 in the WT P2X3 receptor. To this end, starting from the zebrafish P2X4 X-ray structure, we constructed a homology model of the rat P2X3 receptor. The model turned out to be structurally very similar to the template, with a root-mean-square deviation (rmsd) of ∼0.7 Å, as calculated using the structural alignment program SKA.[30] D266 is located in the so-called left flipper region,[4] and it is in contact with the R264 side chain and the NH group of V238 and, potentially, may also interact with a backbone NH group of G277 (Figure 1). For

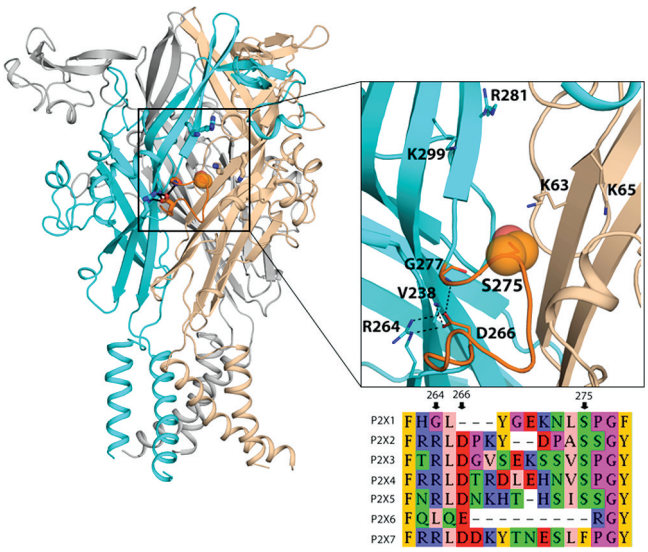

Figure 1. Homology model of the P2X3 receptor (left) along with a binding site region close-up (right). Two adjacent subunits, forming the binding pocket, are colored cyan and beige. A third subunit (colored gray on the left) is not shown on the right for the sake of clarity. The left flipper region is colored orange. Key residues, discussed in the text, are displayed as sticks. The S275 side chain is highlighted using spheres. Plausible polar interactions among V238, R264, D266, and G277 are indicated using dashed lines. The inset shows a multiple-sequence alignment of the left flipper regions of seven rat P2X receptors. Positions of R264, D266, and S275 (P2X3 receptor numbering) are indicated with arrowheads.

the latter, the atom−atom distances in the model are relatively long for the formation of a stable H-bond (∼4 Å between heavy atoms); however, taking into account the relatively low resolution of the template model (3.1 Å), we may not rule out the possibility of this interaction. Thus, it is likely that the D266 side chain stabilizes the position and conformation of the loop (residues 266−277; orange in the Figure 1 structure) within the left flipper region, at least in certain states. Interestingly, this loop, which faces the putative ATP binding pocket, also participates in the subunit−subunit interactions and, thereby, may play an important role in the conformational changes that occur upon agonist binding.

We then analyzed sequences of the left flipper region of all seven rat P2X receptors. Notably, it is one of the most sequence-variable regions (Figure 1, inset) in the multiple-sequence alignment, suggesting that the differences in the amino acid composition in this region and length of the loop may play a role in the differential agonist binding and/or agonist dissociation rates in the various P2X receptors. The S275 residue, identified through visual inspection of the structure of the left flipper region, is present in five of seven P2X receptors and is particularly interesting because it is located at the outer edge of the entrance of the binding pocket (Figure 1). Its polar side chain, which faces the binding site cavity, is likely to play a role in binding of at least some of the P2X agonists, as well to affect agonist dissociation rates. Remarkably, whereas there is an aspartate residue at the position of D266 in the P2X3 receptor, there is an arginine residue (position 264) in the P2X2, -3, -4, -5, and -7 receptors. However, in the P2X2 receptor, which is not prone to desensitization, the left flipper loop is shorter by two positions, which should have an impact on the location of the serine side

dx.doi.org/10.1021/bi200812u | Biochemistry 2011, 50, 8427−8436

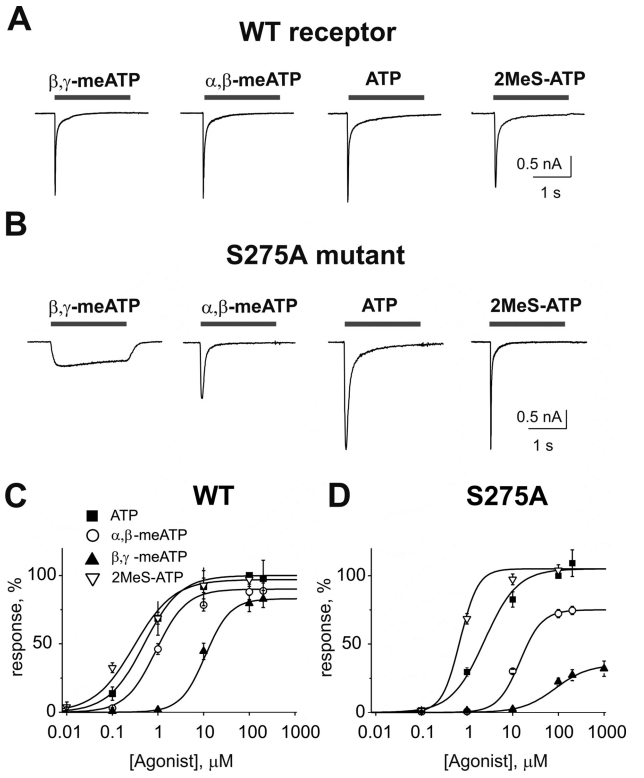

Figure 2. Comparison of different agonists at the WT and S275A receptor. (A and B) Examples of membrane currents generated by the WT (A) or S275 mutant (B) after application of 100 μM β,γ-meATP, α,β-meATP, ATP, and 2MeS-ATP. Note that in the WT all four agents were full agonists generating comparable full size membrane currents, whereas in the S275A mutant only ATP and 2MeS-ATP showed full agonist activity. (C and D) Dose−response curves for the WT (C) and S275A mutant (D). In the WT, the EC_{50} and n_H values were: 0.4 ± 0.1 μM and 0.9 ± 0.1 for 2MeS-ATP, 0.5 ± 0.1 μM and 1.1 ± 0.1 for ATP, 0.9 ± 0.2 μM and 1.3 ± 0.2 for α,β-meATP, and 11.6 ± 2.2 μM and 1.7 ± 0.1 for β,γ-meATP, respectively. For the S275A mutant, the EC_{50} and n_H values were 0.8 ± 0.1 μM and 1.8 ± 0.4 for 2MeS-ATP, 2.4 ± 0.1 μM and 1.2 ± 0.1 for ATP, 14.4 ± 1.2 μM and 1.8 ± 0.2 for α,β-meATP, and 62.9 ± 9.1 μM and 1.5 ± 0.1 for β,γ-meATP, respectively. Data were collected from four to seven cells. Data were normalized to responses induced by 100 μM ATP.

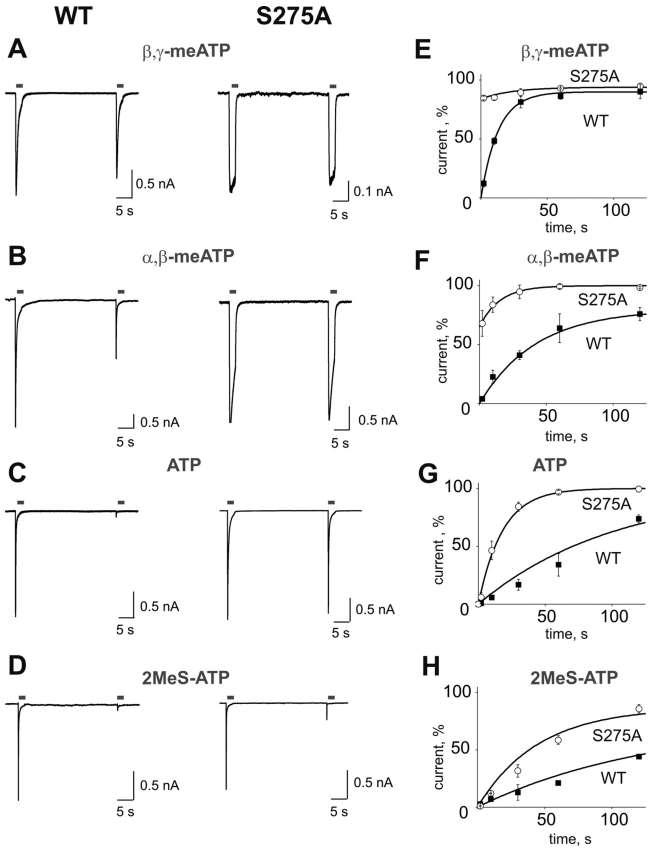

Figure 3. Receptor recovery tested with paired-pulse applications of different agonists to the WT and S275A receptors. (A−D) Paired receptor responses activated by β,γ-meATP, α,β-meATP, ATP, or 2MeS-ATP applied to the WT (left) or S275A receptor (right) with a 30 s interval. (E−H) Time courses of recovery for the WT (■) or S275A receptor (○). Fitting was conducted using the single-exponential function $y = y_0 + Ae^{-(x-x_0)/\tau}$ (for details, see Experimental Procedures). In the WT, the recovery rate constant τ was 13.3 ± 0.9 s for β,γ-meATP, 41.7 ± 3.8 s for α,β-meATP, 102.0 ± 35.1 s for ATP, and 128.7 ± 22.5 s for 2MeS-ATP, while for the S275A mutant, τ was 15.0 ± 1.0 s for α,β-meATP, 18.2 ± 1.8 s for ATP, and 45.3 ± 6.1 s for 2MeS-ATP. Note that the recovery rate was not compared for β,γ-meATP, which generated an almost nondesensitizing response in the S275A mutant (for details, see Experimental Procedures). Data were collected from three to six cells.

chain. In the P2X1 receptor, which, instead, has very strong desensitization properties, this loop is also shorter by three residues but does not have residues R264 and D266, pointing to the possibility that the conformation of this region might be different, which should potentially lead to a differential sensitivity to agonists.

Comparison of Different Agonists at the WT and S275A Receptor. Because our modeling approach suggested the possible key role of S275 in shaping the periphery of the binding site, we created the S275A mutant and tested its activity using a whole cell patch clamp technique.

First, we compared the potency and efficiency of four different agonists at the WT and S275A receptors. Panels A and B of Figure 2 show examples of the inward currents, activated by four full P2X3 agonists, such as β,γ-meATP, α,β-meATP, ATP, and 2MeS-ATP (all at maximal concentrations of 100 μM). Panels C and D of Figure 2 show the dose−response curves for an extended range of concentrations of these agonists (n = 4−7 cells). In the WT receptor, the order of agonist potencies was similar to that previously reported:[29] 2MeS-ATP (EC_{50} = 0.4 ± 0.1 μM) > ATP (EC_{50} = 0.5 ± 0.1 μM) > α,β-meATP (EC_{50} = 0.9 ± 0.2 μM) > β,γ-meATP (EC_{50} = 11.6 ± 2.2 μM). The substitution of serine at position 275 with alanine led to significant changes in agonist potency. The EC_{50} values were shifted to the higher concentrations for all agonists, indicating reduced potency: 2MeS-ATP (EC_{50} = 0.8 ± 0.1 μM) > ATP (EC_{50} = 2.4 ± 0.1 μM) > α,β-meATP (EC_{50} = 14.4 ± 1.2 μM) > β,γ-meATP (EC_{50} = 62.9 ± 9.1 μM). Thus, in the S275A mutant, the increases in EC_{50} were 5.5-, 16-, 5-, and 2-fold for β,γ-meATP, α,β-meATP, ATP, and 2MeS-ATP, respectively (Figure S2A of the Supporting Information).

Notably, unlike the WT, with which all four compounds demonstrated full agonist activity, in the S275A mutant, only ATP and 2MeS-ATP remained as full agonists (Figure 2D). Currents induced by β,γ-meATP showed the most dramatic reduction in amplitude (77.6 ± 2.8%) at 100 μM compared to responses induced by 100 μM ATP (n = 6; P < 0.05). Likewise, α,β-meATP was unable to produce maximal currents [reduction of the amplitude by 27.7 ± 3.0% at 100 μM

dx.doi.org/10.1021/bi200812u | Biochemistry 2011, 50, 8427−8436

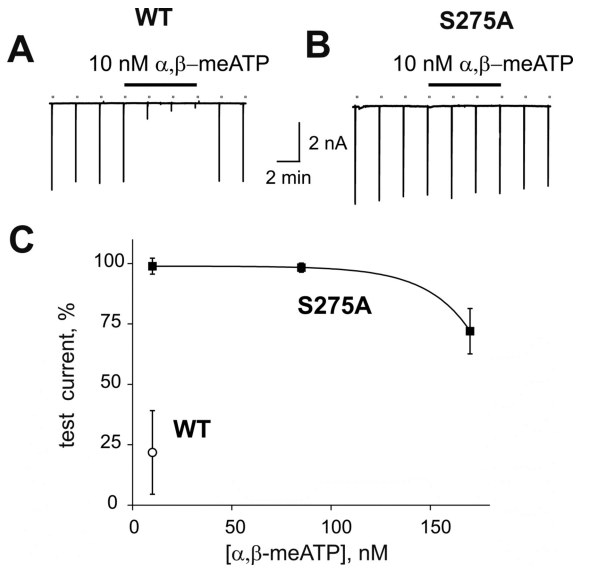

Figure 4. Comparison of the high-affinity desensitization at the WT receptor and S275A mutant (HAD1). (A and B) Effect of 10 nM *α,β*-meATP (black bar) applied after the fourth test currents to the WT (A) or the S275A mutant (B). Test responses were generated with 100 *μ*M *α,β*-meATP. Note the strong inhibition of currents in the WT but the lack of inhibition (HAD1) in the S275A mutant. (C) Dose–response curve for HAD1 in the S275A mutant induced with various concentrations of *α,β*-meATP (■). For comparison, the strong inhibitory action (HAD1) of 10 nM *α,β*-meATP on the WT is shown (○). Note that on the S275A mutant the effective concentration of the agonist to induce HAD1 has been shifted to higher concentrations. Data were collected from five to eight cells.

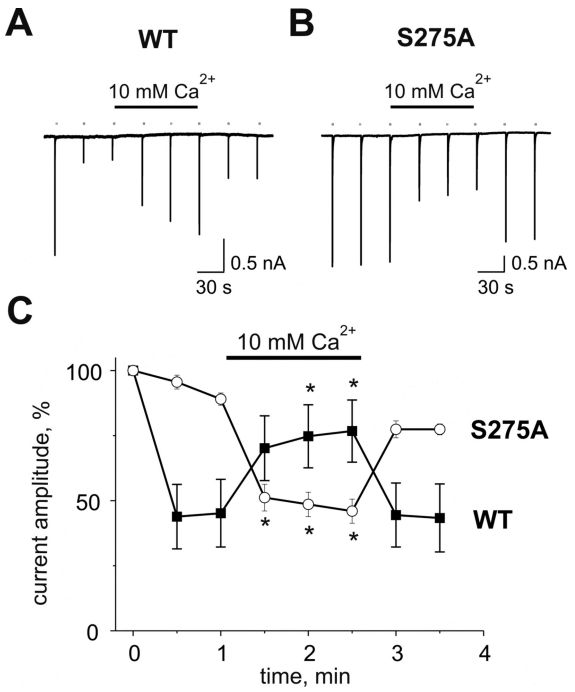

Figure 5. Ca^{2+} differentially modulates the function of the WT and S275A mutant receptor. (A and B) Modulatory effects of 10 mM Ca^{2+} applied to the WT receptor (A) or S275A mutant (B). Note the strong facilitation of currents in the WT receptor contrasting to the inhibition observed, after the same treatment, with the S275A mutant. (C) Time course of changes in the amplitude of currents generated by the WT receptor or S275A mutant in the absence and presence of elevated concentrations of calcium ions. Data were collected from four to six cells. *$P < 0.05$.

compared to responses induced by 100 *μ*M ATP ($n = 7$; $P < 0.05$) (Figure 2D)].

Thus, substitution of serine with alanine at position 275 essentially diminished potency and reduced efficacy for two agonists, *α,β*-meATP and *β,γ*-meATP.

Desensitization Properties of the S275A Mutant. In the WT receptor, current responses peaked and decayed back to the baseline during a 2 s application of all four agonists, indicating fast and complete receptor desensitization (Figure 2A). Unlike the WT, in the S275A receptor dramatic changes in desensitization rate were observed. For all four agonists, current decay was slower in the S275A mutant (longer desensitization onset) than in the WT receptor (Figure 2B). However, this effect was differently presented with different agonists. Thus, the current induced in the S275A mutant with 100 *μ*M *β,γ*-meATP showed almost no desensitization (Figure 2B). The rise time was selectively increased for *β,γ*-meATP by 2-fold ($P > 0.05$; $n = 5$) and for *α,β*-meATP 6-fold ($P > 0.05$; $n = 14$), while it was not changed for ATP or 2MeS-ATP [$P > 0.05$ for both cases (Figure S2B of the Supporting Information)]. On average, mutation slowed the onset of desensitization (judging from the decay rate at a concentration of 10 *μ*M for all agonists) >1000-fold for *β,γ*-meATP ($n = 6$), 13-fold for *α,β*-meATP ($n = 10$), 2-fold for ATP ($n = 8$), and 3-fold for 2MeS-ATP ($n = 8$) (Figure S2C of the Supporting Information).

A paired-pulse protocol at 2, 10, 30, 60, and 120 s intervals was used to compare the receptor recovery after desensitization for different agonists in the WT and S275A receptor. Panels A–D of Figure 3 show that in the WT the recovery obtained with the 30 s interval was much faster for *β,γ*-meATP, moderate for *α,β*-meATP, and very slow for ATP or 2MeS-ATP. In the S275A mutant, recovery was accelerated compared with that of the WT. Recovery rate constants were significantly faster ($P < 0.05$) for *α,β*-meATP, ATP, and 2MeS-ATP (Figure 3E–H; see the figure legend for numeral values of rate constants). In the case of *β,γ*-meATP, the exceptionally minimal level of desensitization in the S275A mutant did now allow this analysis (see Experimental Procedures for detail).

These data indicated that S275 plays an important role in receptor function by maintaining the high rate of onset of desensitization and slowing receptor recovery.

High-Affinity Desensitization of the S275A Mutant. To study the impact of the serine mutation on high-affinity desensitization (HAD), which represents receptor inactivation by underthreshold (nanomolar) agonist concentrations, we used two different protocols.

First, we used the protocol suggested by Pratt et al.,[21] in which HAD was evaluated during the repetitive agonist application (here called "HAD1"). To this end, receptor sensitivity was tested every 2 min by repeated 2 s applications of 10 *μ*M *α,β*-meATP and a nanomolar agonist concentration was applied between test pulses. Figure 4A shows that application of 10 nM *α,β*-meATP after the fourth repetitive test current reduced the next response by 77.1 ± 17.0% ($P < 0.05$; $n = 5$). Unlike the WT receptor, in the S275A mutant the application of 10 nM *α,β*-meATP did not induce any HAD1 (1.1 ± 3.3% change; $P > 0.05$; $n = 6$) (Figure 4B). Likewise, in the WT, the more potent HAD inducer ATP,[7] when applied at 1 nM, induced depression of test responses by 57.8 ± 4.5% ($P = 0.001$; $n = 8$). In the S275A mutant, 1 nM ATP did not induce HAD1 (3.4 ± 2.5% change; $P > 0.05$; $n = 6$).

dx.doi.org/10.1021/bi200812u | *Biochemistry* 2011, 50, 8427–8436

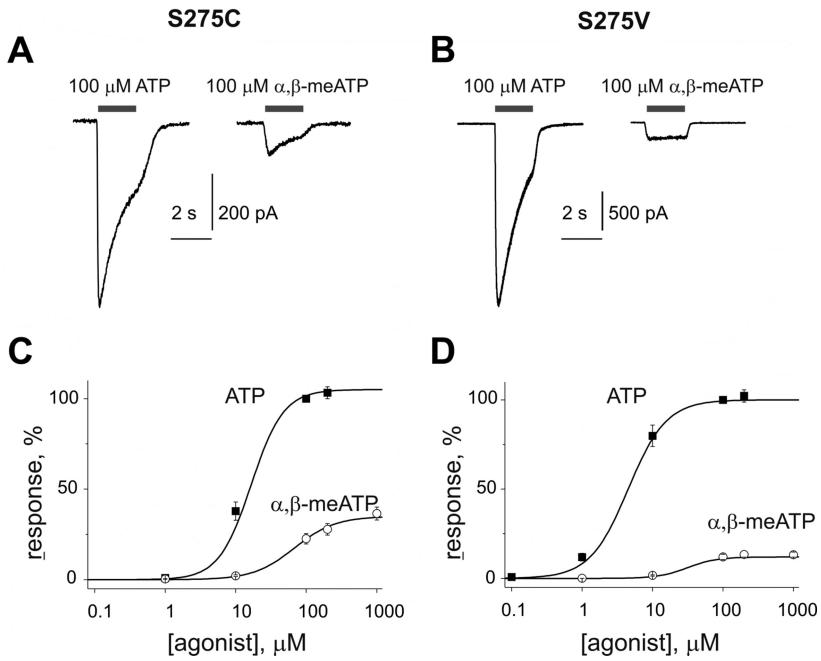

Figure 6. Effect of substitution of S275 with nonpolar cysteine or valine. (A and B) Example of currents generated by the S275C (A) or S275V (B) mutant after application of 100 μM ATP or α,β-meATP. Note that α,β-meATP induced much smaller currents than ATP. (C and D) Dose–response curves for ATP or α,β-meATP with the S275C (C) or S275V (D) mutant. For the S275C mutant, the EC_{50} was 16.6 ± 3.7 μM (n_H = 1.9 ± 0.3) for ATP, while for α,β-meATP, the EC_{50} was 68.4 ± 10.9 μM (n_H = 1.5 ± 0.1). In the S275V mutant, the EC_{50} for ATP was 4.5 ± 0.9 μM (n_H = 1.6 ± 0.1), while for α,β-meATP, the EC_{50} was 31.4 ± 5.4 μM (n_H = 2.1 ± 0.3). Data were normalized to responses induced by 100 μM ATP. Data were collected from five cells.

Second, we tested the HAD of resting receptors (HAD2) that already recovered from previous desensitization.[29] In this case, to evaluate the HAD2, 10 nM α,β-meATP was applied for 90 s after a 6 min resting period. Consistent with previous results[29] for the WT, the depressant effect was 33.4 ± 11.8% [P = 0.008; n = 9 (Figure S3A,E of the Supporting Information)], while in the S275A mutant, 10 nM α,β-meATP induced no changes [2.3 ± 5.1% change; P > 0.05; n = 7 (Figure S3B,E of the Supporting Information)].

Because serine substitution essentially reduced the potency of the S275A mutant, we also tested the action of 170 nM α,β-meATP in both HAD protocols. The conditioning agonist α,β-meATP at this increased concentration induced HAD1 in the S275A mutant by only 28.0 ± 9.4% [P < 0.05; n = 7 (Figure S3C,F of the Supporting Information); the dose–response curve for HAD1 is shown in Figure 4C]. Interestingly, 170 nM α,β-meATP was completely inefficient in the HAD2 protocol [4.5 ± 1.9% change; P > 0.05; n = 7 (Figure S3D,F of the Supporting Information)].

Thus, application of two agonists showed that the S275A mutant had dramatically reduced sensitivity to the inhibitory action of low nanomolar agonist concentrations.

Extracellular Ca^{2+} Differentially Modulates the WT and S275A Mutant. A specific property of P2X3 subunit-containing receptors is their facilitation by extracellular calcium ions.[31] Because in the left flipper region of the P2X3 receptor residue D266, neighboring S275, was involved in Ca^{2+} sensitivity,[16] we tested the action of extracellular calcium on the function of the S275A mutant. In the WT receptor, we confirmed the previously shown[14,31] facilitatory action of 10 mM Ca^{2+} on α,β-meATP-induced membrane currents (Figure 5A,C). Surprisingly, in the S275A mutant, application of 10 mM Ca^{2+} induced a depressant effect instead of facilitation (Figure 5B,C). This inhibitory action (51.5 ± 4.7%; n = 6; P < 0.05) resembled the fast depressant action of calcium ions on P2X2 receptors[17] because with co-application of 10 mM calcium and the agonist α,β-meATP, there was a clear trend to the depressant effect (by 29.4 ± 10.1%; n = 4; P = 0.11) of this divalent cation on membrane currents.

Thus, the substitution of a single amino acid in the left flipper region was sufficient to switch from calcium-induced facilitation to the inhibition of the P2X3 receptor.

Effect of Substitution with Cysteine and Valine. To test the effect of nonpolar amino acids at position 275 in agonist trapping, we substituted serine with cysteine and valine, which both have hydropathy indexes higher than that of alanine.[32] In the S275C mutant, we found that changes in potency, efficacy, and desensitization were more pronounced than in the S275A mutant. While responses to the natural agonist ATP were modestly reduced (23.4 ± 2.1% from the WT value; n = 10; P < 0.05), the agonist α,β-meATP lost its activity dramatically (Figure 6A). Even at a high concentration of 100 μM, this agonist generated only small currents with very weak desensitization (Figure 6A,B). The recovery from desensitization was very fast (67.3 ± 3.2 and 82.8 ± 2.9% at a 10 s interval for ATP and α,β-meATP, respectively; n = 10). Like with the S285A mutant, extracellular calcium (10 mM) quickly inhibited currents induced by α,β-meATP (Figure S4 of the Supporting Information).

In the S275V mutant, the reduced potency and efficacy were also more pronounced than in the S275A mutant (Figure 6C,D). Note that α,β-meATP induced only very small nondesensitizing currents (Figure 6C). While the onset of desensitization with this agonist was exceptionally slow, the recovery was very fast (96.9 ± 1.5% at a 30 s interval; n = 8).

dx.doi.org/10.1021/bi200812u | Biochemistry 2011, 50, 8427–8436

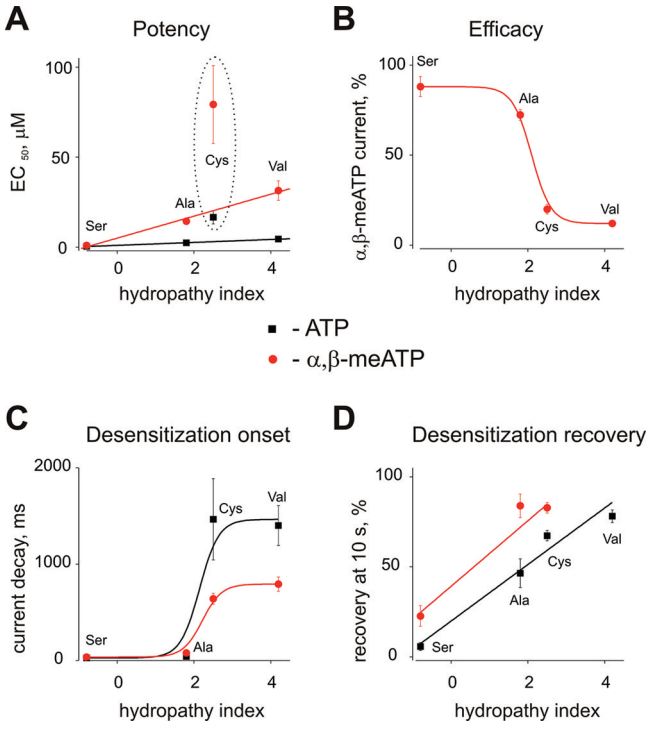

Figure 7. Effect of nonpolar amino acids at position 275 on P2X3 receptor properties. (A) Changes in the potency for ATP (black squares and line) or α,β-meATP (red circles and line) as a function of the hydropathy index. Linear fitting was used for EC_{50} data obtained from S275 (Ser), S275A (Ala), and S275V (Val) receptors. Note that the EC_{50} for S275C (Cys) does not fit this trend (surrounded by a dotted line). (B) Sigmoid curve connecting data of peak currents induced by 100 μM α,β-meATP in the S275, S275A, S275C, and S275V forms. Data are normalized to responses induced by 100 μM ATP. (C) Onset of desensitization (measured as the rate constant of current decay) in the S275, S275A, S275C, and S275V forms as a function of the hydropathy index. (D) Desensitization recovery (measured at a 10 s interval as a percentage of the first test current) in the S275, S275A, S275C, and S275V forms as a function of the hydropathy index. Note the linear character of the fitting function. Data were collected from 4–10 cells.

The summary of results obtained with various substitutions of S275 with nonpolar amino acids is presented in Figure 7. While in the range of serine, alanine, and valine mutants the potency was linearly reduced (Figure 7A), proportionally with respect to hydrophobic properties, the mutation to cysteine more greatly reduced potency than mutation to valine (while the hydropathy index of cysteine is less than that of valine). Similar results were obtained with the two different agonists, ATP and α,β-meATP (Figure 7A). The efficacy of α,β-meATP (measured as the fraction of responses to 100 μM ATP in the same cells) was reduced in the range of serine, alanine, cysteine, and valine, with a steep drop for the two most hydrophobic amino acids (Figure 7B). The rate of onset of desensitization was reduced monotonically, while resensitization was accelerated almost linearly, correlating with hydropathy indexes (Figure 7C,D).

Taken together, these results suggested potential polar interactions between the S275 side chain and the agonist molecule.

Kinetic Modeling of the S275A Mutant. The aim of kinetic modeling was to understand mechanisms underlying the key properties of the P2X3 receptor with the S275A mutation, namely, decreased potency, slow activation and desensitization, fast resensitization, and minimal HAD. Several kinetic models were suggested recently for exploring the function of P2X receptors.[19,33,34] In our study, we used our previously published cyclic kinetic model[20] in which the activation and recovery from desensitization are separated (Scheme 1). Using this approach, we first modeled membrane currents activated by α,β-meATP in the WT receptor (Table 1 and Figure S5A and Table S1 of the Supporting Information). The decreased potency of the S275A mutant was simulated by decelerated agonist binding. To equilibrate the free energy distribution between all bounded and unbounded states, it was also necessary[35] to decelerate other binding steps for resting (R) and desensitized (D) states and accelerate all reverse transitions. These changes slowed receptor activation, accelerated recovery, and largely reduced the level of HAD, simulating our experimental observations with the S275A mutant (Table 1). Because experimental currents on the S275A mutant decayed much slower in the presence of α,β-meATP, we also suggested decelerated O to D transitions (see smaller rate constants for the corresponding transition in Table S1 of the Supporting Information). Thus, we reproduced five of six experimental criteria typical for the S275A mutant (rise time also greatly increased from 26 ± 3.5 to 165 ± 18 ms while in the model it was 250 ms). Figure S5B of the Supporting Information shows an example of the experimental current generated by the S275A mutant overlaid with a simulated current.

In summary, our modeling results were consistent with the view that, in the WT P2X3 receptor, S275 mainly stabilizes all agonist-bound receptor states. This is consistent with the homology modeling results showing that S275 is an important structural element of the agonist binding site.

DISCUSSION

In this study, using a homology model of the rat P2X3 receptor, we identified the S275 residue, located in the left flipper region within the ectodomain, as one of the important contributors to the agonist-binding pocket. Consistent with our predictions, functional testing of several mutants of S275 confirmed an important role of this residue in shaping receptor desensitization and sensitivity to various ATP analogues. Kinetic modeling reproduced the main experimental observations and indicated a key role of S275 in association of the agonist with and dissociation of the agonist from the P2X3 receptor.

Analysis of the Structural Role of D266 Predicts a New Contributor to the Left Flipper. Our previous study identified the important role of the left flipper D266 residue in the agonist sensitivity and desensitization of the P2X3 receptor.[16] However, in the pre-X-ray structure period, this observation was not supported by mechanistic explanations. Now, using the homology model (Figure 1), we suggest that the D266 residue is a stabilizer of the conformation and position of the loop (residues 266–277, orange) within the left flipper region. The left flipper is a part of the putative binding pocket and also participates in the subunit–subunit interactions.[4] Thus, this region, upon agonist binding, potentially may propagate conformational changes to the subunit interface, which should finally lead to the changes in the transmembrane region and opening of the ion channel.

While exploring in silico the functional role for D266, we identified the S275 residue, the polar residue in the left flipper loop located near the entrance of the putative binding pocket,[4] which also faces the binding cavity. We proposed that this side

dx.doi.org/10.1021/bi200812u | Biochemistry 2011, 50, 8427–8436

Table 1. Comparison of Experimental versus Modeling Results[a]

criterion (with 10 μM α,β-meATP)	experimental WT	model WT	experimental S275A	model S275A
rise time (ms)	26 ± 3.5	27	165 ± 18	250
decay time (ms)	86 ± 7.3	84	1098 ± 142	1030
EC_{50} (μM)	0.9 ± 0.2	1.0	14.4 ± 1.2	15
% recovery from desensitization at 30 s	41 ± 3.75	42	95 ± 5.75	98
% inhibition by 10 nM α,β-meATP with previous desensitization (HAD1)	78 ± 17	66	1 ± 3	2
% inhibition by 10 nM α,β-meATP without previous desensitization (HAD2)	33 ± 11	33	2 ± 5	1

[a]Explanation in the text.

chain played an important role in the binding of various P2X3 agonists. It is also worth noting that a very recent study identified a couple of residues (N140 and L186; P2X2 receptor numbering) as being important for ATP binding.[13] Interestingly, F174 in the P2X3 receptor (corresponds to L186 in the P2X2 receptor) is in direct contact with S275 in our model.

S275 and Full Agonists of the P2X3 Receptor. P2X3 receptors are activated with various full agonists,[19,20,29] including α,β-meATP, which is active at only P2X1 and P2X3 receptors.[5] Consistent with this, we found that four agonists with different chemical structures (β,γ-meATP, α,β-meATP, ATP, and 2MeS-ATP) were fully active at the WT receptor. In the S275A mutant, EC_{50} values increased for all agonists; however, only ATP and 2MeS-ATP remained full agonists, while β,γ-meATP and α,β-meATP became partial agonists. Tests with α,β-meATP performed on hydrophobic surrogates S275C and S275V indicated an even greater decrease in efficacy for this agonist. Thus, it is likely that the side chain of S275 plays an important role in ligand binding, most critically with β,γ-meATP and α,β-meATP, which is consistent with the location of several positively charged residues identified in previous studies (Figure 1), involved in agonist binding.[3,5] Notably, unlike S275, the neighboring S269 apparently does not play a role in agonist sensitivity,[36] which is in agreement with its location in the structural model at the surface of the protein.

Along with changes in the EC_{50} values and greatly reduced efficacy for certain agonists, we also observed that in the S275A mutant, the rise time of membrane currents activated by β,γ-meATP or α,β-meATP was slower than in the WT receptor. Like changes in EC_{50}, this can be attributed to weaker agonist binding or faster dissociation. Thus, one could hypothesize that in the receptor, which lacks the side chain of S275, it takes "longer" to fix β,γ-meATP and α,β-meATP in the binding pocket and to propagate conformational changes to the transmembrane region for channel opening. The common mechanisms underlying the parallel changes in EC_{50}, efficacy, and current rise time were confirmed in the kinetic modeling of the P2X3 receptor.

S275 and Desensitization Properties of the P2X3 Receptor. An even more striking difference between the WT and the S275A mutant was observed with receptor desensitization. In the S275A mutant, the desensitizing ability was diminished for all tested agonists, which quickly and completely desensitized the WT receptor. The most extreme effect was observed with β,γ-meATP, which generated currents virtually lacking desensitization even at a high concentration of 100 μM. This weak agonist activity of the S275A mutant was probably due to slow binding and/or fast dissociation. Likewise, a slow onset of desensitization and accelerated resensitization were observed with S275C and S275V mutants with ATP and α,β-meATP.

The estimation of dissociation of the agonist from the receptor is normally not easy to measure with the electrophysiological techniques. However, in the case of P2X3 receptors, agonist dissociation is a rate-limiting step in exceptionally slow recovery from desensitization,[20,21,29,33] and therefore, the rate of dissociation of the agonist from desensitized receptors could be estimated using a paired-pulse protocol.[29] Using such a protocol, we found that the recovery from desensitization was much faster in the S275A mutant, indicating that agonist dissociation is faster when the left flipper is modified due to the lack of the side chain of S275. We suggest that in the WT receptor, the agonist is normally trapped by the left flipper region at the entrance to the binding pocket. Thus, the left flipper loop could serve as a "cap", in which the side chain of S275 is likely in contact with the ligand molecule, preventing its fast dissociation. When we substitute serine with alanine, we reduce the efficiency of the cap because we remove a polar group that might be responsible for forming an H-bond with the agonist. By introducing more hydrophobic and bulkier amino acids like cysteine or valine, we probably also add steric clashes with certain agonists, like α,β-meATP, which explains such a significant decrease in the efficacy observed with mutants S275C and S275V.

In the context of a hypothesis that the side chain of S275 serves as a cap for the binging pocket, we found that the level of not only classical desensitization but also HAD was largely reduced in the S275A mutant. HAD was almost absent in the mutant, suggesting that the nanomolar agonist is not being captured in the pocket.

Effect of Ca^{2+} on the Left Flipper Mutants. Surprisingly, we found that the substitution of a single serine with alanine at position 275 was sufficient for switching from original facilitation to the inhibition of the ATP-gated P2X3 receptor by calcium ions. Specific facilitation of P2X3 receptors by extracellular calcium was discovered by Cook and McCleskey[14,31] and was confirmed in several later publications.[15,16] Previously, we found that substitution of alanine for D266 in the left flipper region virtually abolished Ca^{2+} sensitivity.[16] Now we show an even stronger effect of a single amino acid substitution within the left flipper, when instead of facilitation, treatment with calcium ions inhibits the function of the S275A mutant. This effect was not specifically linked to alanine, because the similar inhibitory action of the extracellular calcium was also observed with the S275C mutant. While the mechanism of facilitation of P2X3 receptors by extracellular calcium was based on accelerated resensitization,[31] the nature of the inhibitory action remains unknown. Most probably, it is based on a different mechanism that is unmasked when the rate of desensitization in the S275A (or S275C) mutant is largely reduced. In this regard, it is interesting to note that the strong and fast inhibitory effect of calcium ions was observed in P2X2 receptors that are not prone to desensitization.[17] Because

dx.doi.org/10.1021/bi200812u | Biochemistry 2011, 50, 8427–8436

calcium ions allosterically regulate the function of the P2X3 receptor even at physiological concentrations,[15] these data suggest that certain residues in the left flipper region are functioning in a calcium-dependent manner.

CONCLUSION

In conclusion, our data provide a mechanistic explanation for two key residues in the left flipper region of the ectodomain of the P2X3 receptor. One residue (D266) has been characterized previously in the precrystal structure of the P2X receptor period, while the other (S275) was identified in silico in the context of this work. We suggest that the side chain of D266 stabilizes the conformation of a loop within the left flipper region, while S275 in that loop may directly interact with ATP and its analogues, regulating agonist potency, efficacy, and desensitization properties through the control of the association and dissociation rates of the agonists.

ASSOCIATED CONTENT

Supporting Information

An alignment of the modeled regions of the P2X3 and P2X4 receptors (Figure S1), comparison of EC_{50}, rise time, and decay time values of the WT and S275A receptors (Figure S2), HAD1 and HAD2 with various agonist concentrations (Figure S3), fast inhibitory action of Ca^{2+} on membrane currents generated by the S275C mutant (Figure S4), kinetic modeling of the WT and S275A mutant (Figure S5), and rate constants used to simulate membrane currents activated by α,β-meATP (Table S1). This material is available free of charge via the Internet at http://pubs.acs.org.

AUTHOR INFORMATION

Corresponding Author

*Telephone: +358403553665. Fax: +35817163030. E-mail: rashid.giniatullin@uef.fi.

Author Contributions

N.P. and K.K. contributed equally to this work.

Funding

This work was supported by the Finnish Academy (Grant 127150 to R.G.). A.S. was supported by RFBR grants. V.T. was supported by the Grant Agency of Charles University (Grant 3446/201).

ACKNOWLEDGMENTS

We thank Prof. Hana Zemkova for providing the constructs of S275 mutants.

ABBREVIATIONS

α,β-meATP, α,β-methylene-ATP; β,γ-meATP, β,γ-methylene-ATP; EC_{50}, half-maximal effective concentration; HAD, high-affinity desensitization; HEK293, human embryonic kidney; 2MeS-ATP, 2-methylthio-ATP; TM, transmembrane; WT, wild type.

REFERENCES

(1) Burnstock, G. (2001) Purine-mediated signalling in pain and visceral perception. *Trends Pharmacol. Sci. 22*, 225−272.

(2) North, R. A. (2004) P2X3 receptors and peripheral pain mechanisms. *J. Physiol. 554*, 301−308.

(3) Khakh, B. S., and North, R. A. (2006) P2X receptors as cell-surface ATP sensors in health and disease. *Nature 442*, 527−532.

(4) Kawate, T., Michel, J. C., Birdsong, W. T., and Gouaux, E. (2009) Crystal structure of the ATP-gated P2X4 ion channel in the closed state. *Nature 460*, 592−598.

(5) Evans, R. J. (2010) Structural interpretation of P2X receptor mutagenesis studies on drug action. *Br. J. Pharmacol. 161*, 961−971.

(6) Coddou, C., Yan, Z., Obsil, T., Huidobro-Toro, P. J., and Stojilkovic, S. S. (2011) Activation and regulation of purinergic P2X receptor channels. *Pharmacol. Rev. 63*, 641−683.

(7) Roberts, J. A., and Evans, R. J. (2006) Contribution of conserved polar glutamine, asparagines and threonine residues and glycosylation to agonist action at human P2X1 receptors for ATP. *J Neurochem. 96*, 843−852.

(8) Bodnar, M., Wang, H., Riedel, T., Hintze, S., Kato, E., Fallah, G., Gröger-Arndt, H., Giniatullin, R., Grohmann, M., Hausmann, R., Schmalzing, G., Illes, P., and Rubini, P. (2011) Amino acid residues constituting the agonist binding site of the human P2X3 receptor. *J. Biol. Chem. 286*, 2739−2749.

(9) Kracun, S., Chaptal, V., Abramson, J., and Khakh, B. S. (2010) Gated access to the pore of a P2X receptor: Structural implications for closed-open transitions. *J. Biol. Chem. 285*, 10110−10121.

(10) Keceli, B., and Kubo, Y. (2009) Functional and structural identification of amino acid residues of the P2X2 receptor channel critical for the voltage- and ATP-dependent gating. *J. Physiol. 587*, 5801−5818.

(11) Wolf, C., Rosefort, C., Fallah, G., Kassack, M. U., Hamacher, A., Bodnar, M., Wang, H., Illes, P., Kless, A., Bahrenberg, G., Schmalzing, G., and Hausmann, R. (2011) Molecular determinants of potent P2X2 antagonism identified by functional analysis, mutagenesis, and homology docking. *Mol. Pharmacol. 79*, 649−661.

(12) Jiang, R., Martz, A., Gonin, S., Taly, A., de Carvalho, L. P., and Grutter, T. (2010) A putative extracellular salt bridge at the subunit interface contributes to the ion channel function of the ATP-gated P2X2 receptor. *J. Biol. Chem. 285*, 15805−15815.

(13) Jiang, R., Lemoine, D., Martz, A., Taly, A., Gonin, S., de Carvalho, L. P., Specht, A., and Grutter, T. (2011) Agonist trapped in ATP-binding sites of the P2X2 receptor. *Proc. Natl. Acad. Sci. U.S.A. 108*, 9066−9071.

(14) Cook, S. P., and McCleskey, E. W. (1997) Desensitization, recovery and Ca^{2+}-dependent modulation of ATP-gated P2X receptors in nociceptors. *Neuropharmacology 36*, 1303−1308.

(15) Giniatullin, R., Sokolova, E., and Nistri, A. (2003) Modulation of P2X3 receptors by Mg^{2+} on rat DRG neurons in culture. *Neuropharmacology 44*, 132−140.

(16) Fabbretti, E., Sokolova, E., Masten, L., D'Arco, M., Fabbro, A., Nistri, A., and Giniatullin, R. (2004) Identification of negative residues in the P2X3 ATP receptor ectodomain as structural determinants for desensitization and the Ca^{2+}-sensing modulatory sites. *J. Biol. Chem. 279*, 53109−53115.

(17) Virginio, C., North, R. A., and Surprenant, A. (1998) Calcium permeability and block at homomeric and heteromeric P2X2 and P2X3 receptors, and P2X receptors in rat nodose neurones. *J. Physiol. 510*, 27−35.

(18) North, A. (2002) Molecular physiology of P2X receptors. *Physiol. Rev. 82*, 1235−1301.

(19) North, R. A., and Surprenant, A. (2000) Pharmacology of cloned P2X receptors. *Annu. Rev. Pharmacol. Toxicol. 40*, 563−580.

(20) Sokolova, E., Skorinkin, A., Fabbretti, E., Masten, L., Nistri, A., and Giniatullin, R. (2004) Agonist-dependence of recovery from desensitization of P2X3 receptors provides a novel and sensitive approach for their rapid up or downregulation. *Br. J. Pharmacol. 141*, 1048−1058.

(21) Pratt, E. B., Brink, T. S., Bergson, P., Voigt, M. M., and Cook, S. P. (2005) Use-dependent inhibition of P2X3 receptors by nanomolar agonist. *J. Neurosci. 25*, 7359−7365.

(22) Colquhoun, D. (1998) Binding, gating, affinity and efficacy: The interpretation of structure-activity relationships for agonists and of the effects of mutating receptors. *Br. J. Pharmacol. 125*, 924−947.

(23) Sali, A., and Blundell, T. L. (1993) Comparative protein modelling by satisfaction of spatial restraints. *J. Mol. Biol. 234*, 779–815.
(24) Khafizov, K., Staritzbichler, R., Stamm, M., and Forrest, L. R. (2010) A study of the evolution of inverted-topology repeats from LeuT-fold transporters using AlignMe. *Biochemistry 49*, 10702–10713.
(25) Forrest, L. R., Tang, C. L., and Honig, B. (2006) On the accuracy of homology modeling and sequence alignment methods applied to membrane proteins. *Biophys. J. 91*, 508–517.
(26) Laskowski, R. A., Moss, D. S., and Thornton, J. M. (1993) Main-chain bond lengths and bond angles in protein structures. *J. Mol. Biol. 231*, 1049–1067.
(27) Notredame, C., Higgins, D. G., and Heringa, J. (2000) T-Coffee: A novel method for fast and accurate multiple sequence alignment. *J. Mol. Biol. 302*, 205–217.
(28) Chrétien, J. M., and Chauvet, G. A. (1998) An algorithmic method for determining the kinetic system of receptor-channel complexes. *Math. Biosci. 147*, 227–257.
(29) Sokolova, E., Skorinkin, A., Moiseev, I., Agrachev, A., Nistri, A., and Giniatullin, R. (2006) Experimental and modeling studies of desensitization of P2X3 receptors. *Mol. Pharmacol. 70*, 373–382.
(30) Petrey, D., Xiang, Z., Tang, C. L., Xie, L., Gimpelev, M., Mitros, T., Soto, C. S., Goldsmith-Fischman, S., Kernytsky, A., Schlessinger, A., Koh, I. Y. Y., Alexov, E., and Honig, B. (2003) Using multiple structure alignments, fast model building, and energetic analysis in fold recognition and homology modelling. *Proteins 53*, 430–435.
(31) Cook, S. P., Rodland, K. D., and McCleskey, E. W. (1998) A memory for extracellular Ca^{2+} by speeding recovery of P2X receptors from desensitization. *J. Neurosci. 18*, 9238–9244.
(32) Kyte, J., and Doolittle, R. F. (1982) A simple method for displaying the hydropathic character of a protein. *J. Mol. Biol. 157*, 105–132.
(33) Karoly, R., Mike, A., Illes, P., and Gerevich, Z. (2008) The unusual state-dependent affinity of P2X3 receptors can be explained by an allosteric two-open-state model. *Mol. Pharmacol. 73*, 224–234.
(34) Yan, Z., Khadra, A., Li, S., Tomic, M., Sherman, A., and Stojilkovic, S. S. (2010) Experimental characterization and mathematical modeling of P2X7 receptor channel gating. *J. Neurosci. 30*, 14213–14224.
(35) Mitra, A., Tascione, R., Auerbach, A., and Licht, S. (2005) Plasticity of acetylcholine receptor gating motions via rate-energy relationships. *Biophys. J. 89*, 3071–3078.
(36) Stanchev, D., Flehmig, G., Gerevich, Z., Nörenberg, W., Dihazi, H., Fürst, S., Eschrich, K., Illes, P., and Wirkner, K. (2006) Decrease of current responses at human recombinant P2X3 receptors after substitution by Asp of Ser/Thr residues in protein kinase C phosphorylation sites of their ectodomains. *Neurosci. Lett. 393*, 78–83.